Arabian Journal of Geosciences (2022) 15: 1377
https://doi.org/10.1007/s12517-022-10638-w

ORIGINAL PAPER

Modeling and forecasting of rainfall and temperature time series in East Wollega Zone, Western Ethiopia

Teka Bekuma[1] · Girma Mamo[2] · Alemayehu Regassa[1]

Received: 27 December 2021 / Accepted: 19 July 2022 / Published online: 5 August 2022

Abstract

Temperature and rainfall variations have already had an impact on the production of food crops, and upcoming variations pose a potential to further increase food insecurity. Smallholder farmers in Ethiopia rely mostly on rain-fed subsistence agriculture, which is extremely vulnerable to climate change. They forecast weather and climate using indigenous knowledge and their farm expertise to guide their farming operations. Future climate information based on scientific evidence can be obtained at the national or regional level rather than at the local level. Food production is an issue to accommodate rapid population growth due to farmers' reliance on a single rainy season and a lack of dependable climatic projections. The forecasting of temperature and rainfall by researchers can aid farmers in making decisions because both factors have a substantial impact on agricultural production. In order to increase smallholder farmers' capacity for adaptation and establish resilience to climate hazards in East Wollega Zone of Oromia National Regional State, the study focused on forecasting rainfall and temperature. The daily rainfall and temperature data of 37 years (1981–2017) from 7 stations were collected from National Meteorological Agency of Ethiopia. Temperature and rainfall predictions were made using the ARIMA, quadratic trend, linear trend, and simple exponential smoothing models. Accuracy of the models has been determined based on an Akaike information criterion (AIC). Sen's slope estimator was used to determine the magnitude of change, while the Mann–Kendall (MK) test was utilized to examine the trend of forecasted rainfall and temperature. Winter and spring rainfall predictions showed a substantial decreasing and increasing trend, respectively. Summer and autumn rainfall exhibited an insignificant upward and downward trend respectively, but yearly rainfall showed a substantial declining trend. The projected winter, spring, autumn, and yearly minimum temperatures indicate a considerable upward tendency, whereas the summer minimum temperature shows a negligible upward trend. Summer, autumn, and yearly maximum temperatures are expected to fall, but maximum temperatures in winter and spring are expected to rise dramatically. As the livelihoods of the farmers depend on seasonal rain-fed agriculture, adapting to the adverse impact of rainfall and temperature variability is unavoidable. Decisions about the agricultural system and the development of adaptation strategies in the area should consider rising minimum temperatures and declining annual rainfall.

Keywords ARIMA models · Forecast · Climate variability · Rainfall · Temperature

Introduction

Changes in the patterns of climate extremes at global, regional, and local scales have been documented in recent special reports on climate extremes (Omondi et al. 2014). Because of its reliance on agriculture, which is highly susceptible to weather and climate variables, Sub-Saharan Africa has been portrayed as the most vulnerable region to the effects of global climate change (Kotir 2011). Ethiopia is frequently cited as one of the most extreme examples of Africa's vulnerability to future climate change (Conway and Schipper 2011). The majorities of Ethiopians live in rural

Responsible Editor: Zhihua Zhang

✉ Teka Bekuma
tekabeka2017@gmail.com

1 Jimma University, Jimma, Ethiopia

2 Ethiopian Institute of Agricultural Research, Addis Ababa, Ethiopia

areas and rely on rain-fed agriculture (Rosell 2011). Rainfall and temperature patterns are frequently recognized as crucial variables in explaining different socio-economic concerns in Ethiopia, whose economy is mostly dependent on low-productivity rain-fed agriculture (Cheung et al. 2008). It is critical to characterize the seasonal and inter-annual spatial temporal variability of rainfall and temperature in a changing climate in order to identify climate-induced changes and suggest appropriate future adaptation techniques (Wagesho et al. 2013). Climate change and variability are now posing a significant threat to agricultural production for smallholder farmers who rely on rain-fed agriculture on small farms (Workalemahu and Dawid 2021).

Ethiopia offers a vast range of eco-environmental variability, ranging from intense heat at one of the world's lowest points to one of Africa's coolest mountains (Mekasha et al. 2014). Agriculture is the backbone of Ethiopian economy, which contributes 45% to the gross domestic product (GDP), 85% foreign earnings and provides livelihood to 80% of the population (Tesfahun et al. 2018). Climate variability in the form of higher temperature and increased rainfall variability and reduced crop yield has threatened food security in subsistence rain fed–based agriculture (Melese 2019). In Ethiopia, recurrent droughts and floods have been a major and persistent challenge to sustainable food crop production (Muhammad et al. 2021). Climate variability affected crop productivity through delay of onset, early cessation, shortening of growing period, decreasing crop yields, and quality (Singh 2019). Although Ethiopia has different agro-ecologies suited for food crop production, weather-related risks and a lack of a climate monitoring system impede agricultural productivity (Wasihun and Desu 2021). In the coming decades, ensuring food security for the rapidly growing population is one of the greatest challenges in Ethiopia (Gebissa 2021).

The knowledge of past and recent climatic trends such as rainfall and temperature are a pre-requisite for the future sustainability of agriculture and food security (Sintayehu 2018). Climate information is very crucial in supporting smallholder farmers to manage climate related risks and adapt to climate variability (Radeny et al. 2019). Smallholder subsistence farmers are vulnerable to climate change impacts due to their low adaptive capacity, dependence on rain-fed agriculture, widespread poverty and lack of reliable weather and climate information in Ethiopia (Musayev et al. 2021). Rainfall and temperature variability has imposed formidable uncertainties and risks in food crop production, thus forecasting for the future provides an opportunity to deal with such risks in advance (Yate and Hutjes 2021). Prediction of rainfall and temperature in advance would have enormous environmental, social, and economic benefits to countries such as Ethiopia that depend on rain-fed agriculture (Diro et al. 2008).

In Ethiopia, particularly in the study area, farmers depend on their accumulated experience for weather prediction to plan their farming activity (Wagaye et al. 2020). Developing more reliable and accessible climate information can assist smallholder farmers to improve their adaptive capacity and building resilience to climate risk (Gbangou et al. 2020). Forecasting temperature and rainfall is an important for planning and formulating of agricultural adaptation strategies (Teshome 2020). Subsistence rain-fed agriculture remains the main source of livelihoods in the study area facing challenge to feed the rapidly growing population because of climate variability. Thus, the study aimed at forecasting rainfall and temperature to provide information on for adaptation planning in advance. The objectives of the study were (1) to provide farmers with future climate data that they can utilize to lessen the risk of crop losses due to weather and (2) to determine the future rainfall and temperature trends in the research area. Rainfall and temperature have a significant impact on the agriculture. Farmers in the study area forecast weather and climate using indigenous knowledge and their acquired farm experience to guide their farming activities. Accurate future climate information can assist farmers in making more educated decisions about their farming operations. Climate information that is accurate and dependable is becoming increasingly significant, especially in the field of rain-fed agricultural production. Having access to scientific data can assist farmers in making adjustments to their farming activities and planning for adaptation ahead of time. Therefore, the study is highly significant for the study area.

Materials and methods

Description of the study area

The study was conducted in East Wollega Zone of Oromia National Regional State, Western Ethiopia. It is one of the Zones in Oromia National Regional State comprising 17 rural districts and 289 rural peasant associations. It is located at 328 km west of Addis Ababa. The total land area of the zone is about 14,102.5km^2 which accounts for about 3.88% of the total area of the Oromia National Regional State (EWZPEDO 2017). East Wollega Zone is found on Northing 8°31′20″N to 10°22′30″N and Easting 36°06′00″E 37°12′00″E. It is bordered by Amhara National Regional State in the North, Jimma zone in the South, Horo Guduru Wollega and West Shewa zone in the East, Benishangul Gumuz National Regional State in the North–West, West Wollega zone in the West, and Buno Bedelle zone in the South West. It is located at 328 km of west of Addis Ababa, the capital city of Ethiopia (EWZPEDO 2017). Figure 1 below shows location map of the research area.

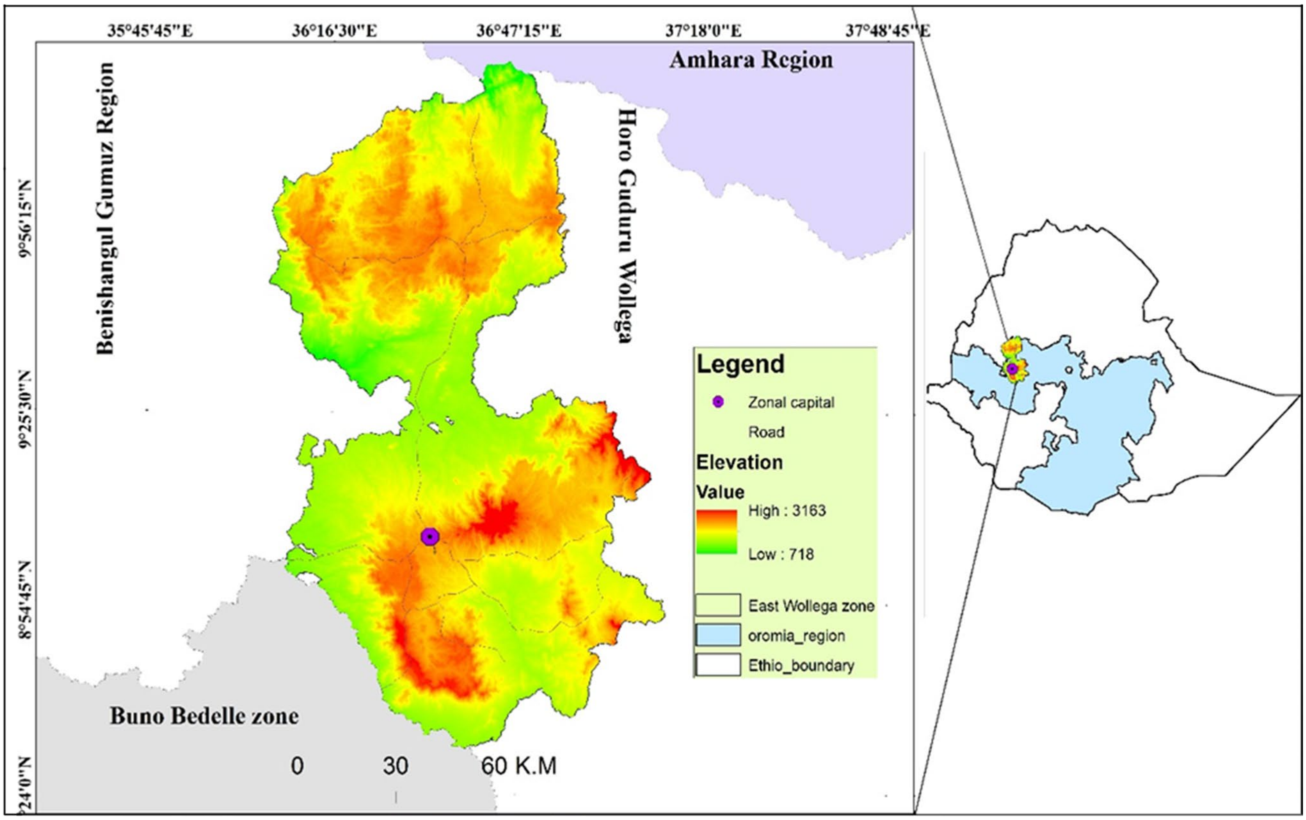

Fig. 1 Location map of the research area

Topography and climate

The altitude of the zone ranges between 718 and 3163 masl. It is mainly of low plateau with some isolated ranges such as in Jima Arjo district. The climate of the zone is divided into three categories, namely highland 20.50%, midland 50.90%, and lowland 28.60%. The annual temperature is between 14 to 25 °C and annual rain fall is also between 1000 and 2400 mm (EWZPEDO 2017). Maximum rainfall is received from June to August. The climatic condition alternates with long summer rainfall (June to September), short rain season (March to April), and winter dry seasons (December to February). The minimum and maximum annual rainfall and daily temperature ranges from 1450 to 2150 mm and 15 to 27 °C, respectively (Asamenew and Mezene 2015). The major rainy season is during the months of June to September which is the case for many Ethiopian highlands (Fita 2014).

Socio-economic conditions

Population

According to East Wollega Zone Planning and Economic Development Office (EWZPEDO 2017) East Wollega zone's total population was 1,628,569 out of which 824,195 (50.61%) were males whereas about 804,374 (49.39%) were females. During this year, about 81.12% of the total populations were rural, who are directly engaged in agriculture. During the year 2017, there were 175,173 males and 20,405 females totally 195,578 households in peasant associations of the zone. The crude population density of the zone in the year 2017 was 115.034 person per km^2 (EWZPEDO 2017). Rapid human growth in the study area has resulted in a significant shift in land use, with the majority of natural forest destroyed for cereal cultivation and local fuel (Achalu 2014).

Farming system

The farming system in the study region is characterized as mixed farming (Degefa et al. 2020). Crop cultivation and livestock keeping are the primary sources of income in the study area. Crop and livestock production are used for both domestic use and as a source of revenue. Maize, sorghum, teff, millet, wheat, and barley are the principal cereal crops farmed in the area. Crop production is a major source of income for farmers, and it is primarily rain-fed agriculture. In 2017, the zone had 315,752 ha of cultivated land and produced 11,733,199 quintals of grains. Temperature, length of growing season, moisture availability, flood hazard, soil degradation, toxicity, and rooting condition are some of the primary characteristics that define the land's potentiality (EWZPEDO 2017). Cattle rearing relies on natural grasses and crop residues that are retained in the traditional management approach (Dereje et al. 2014). Land degradation, erosion, variable rainfall distribution, small land holdings and fragmentation, traditional agricultural operations, and a lack of access routes to local or central markets are the main obstacles to agricultural productivity in the zone. In addition, inefficient and insufficient irrigation schemes, a low emphasis on the market system and lack of infrastructure, lack of finance facilities, as well as a lack of technical support, are some of the issues that limit agricultural output (EWZPEDO 2017).

Data type and sources

Historical time series climate data (temperature and rainfall) for 37 years of 7 stations (1981–2017) was collected from National Meteorology Agency (NMA). The study included both dependent and independent (explanatory) variables. In this case, time was used as independent variable and temperature and rainfall as the dependent variables.

Analytical methods

An autoregressive integrated moving average (ARIMA), trend, and simple exponential smoothing models were used for prediction of rainfall and temperature time series. After automatically running 17 different models for each variables using Statgraphics Centurion version 19 statistical software, the best models were selected for forecasting the variables (Fig. 2). The selections of the models were based on the smallest value of the Akaike information criterion (AIC) for prediction. Akaike information criteria (AIC) is an important tool for model selection (Acquah 2018). Models with minimum AIC values are preferred. Akaike's (1973) information criterion (AIC) is defined as:

$$\mathrm{AIC} = -2(\log - \mathrm{likelihood}) + 2K$$

where K is the number of model parameters (the number of variables in the model plus the intercept). Log-likelihood is a measure of model fit.

Mann–Kendall trend test and Sen's slope estimator

Mann–Kendall (MK) test was employed to examine the trend of forecasted rainfall and temperature. Kendall's tau, S statistics, and P value were used to detect variation in rainfall and temperature. The P values used to determine whether any apparent patterns are statistically significant or not. The decision was made based on level of significance (alpha value of 0.05) which compared against the p value. There is no significant trend if the p value is above the significance level (alpha value of 0.05); there is a significant trend if the p value is below the significance threshold. The negative of MK Stat (S) and Kendall's tau value represents the declining trend while the positive value represents the increasing trend. Sen's slope estimator was used to estimate the average changes in the forecasted rainfall and temperature over time.

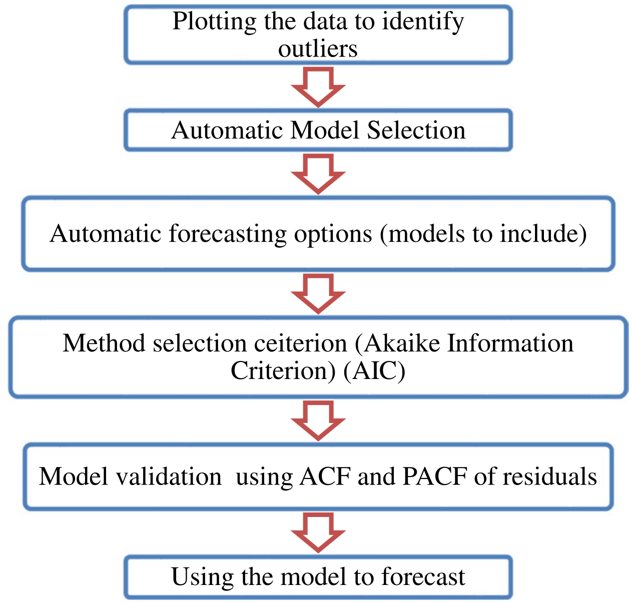

Fig. 2 Process of automatic model selection using Statgraphics Centurion statistical software

Results and discussion

Winter rainfall time series forecasting

To forecast future values of winter rainfall, an autoregressive integrated moving average (ARIMA) model was selected. The output summarizes the statistical significance of the terms in the forecasting model. Terms with P values less than 0.05 are statistically significantly at the 95% confidence level. Table 1 below indicates ARMA model summary.

Forecast plot of winter rainfall using ARIMA (0, 2, 2) model

Figure 3 below indicates forecasted plots of winter rainfall. Figure 3A indicates time sequence plot for winter rainfall with the predicted values when the actual data available from the fitted models. Figure 3B indicates forecasted plots

Table 1 ARIMA (0, 2, 2) model summary to forecast winter rainfall

Parameter	*Estimate*	*Stnd. error*	*t*	*P value*
MA(1)	1.78815	0.0434824	41.1235	0.000000
MA(2)	−0.80379	0.042733	−18.8096	0.000000

Table 2 Quadratic trend model summary to forecast spring rainfall

Parameter	*Estimate*	*Stnd. Error*	*t*	*P value*
Constant	476.801	55.7966	8.54535	0.000000
Slope	−19.2423	6.77106	−2.84184	0.007529
Quadratic	0.495809	0.172823	2.86888	0.007031

of winter rainfall and for time periods beyond the end of the series shows 95% prediction limits for the forecasts. These limits show where the true data value at a selected future time is likely to be with 95% confidence.

Spring rainfall time series forecasting

To forecast future values of spring rainfall, a quadratic trend model was selected. This model assumes that the best forecast for future data is given by a quadratic regression curve fit to all previous data. The output summarizes the statistical significance of the terms in the forecasting model. Terms with *P* values less than 0.05 are statistically significantly at the 95% confidence level. In this case, the *P* value for the quadratic term is less than 0.05, so it is significantly significant. Table 2 below shows a quadratic trend model summary.

Forecast plot of sprig rainfall using Quadratic trend model

Figure 4 below indicates forecasted plots of spring rainfall. Figure 4A shows time sequence plot for spring rainfall with the predicted values when the actual data available from the

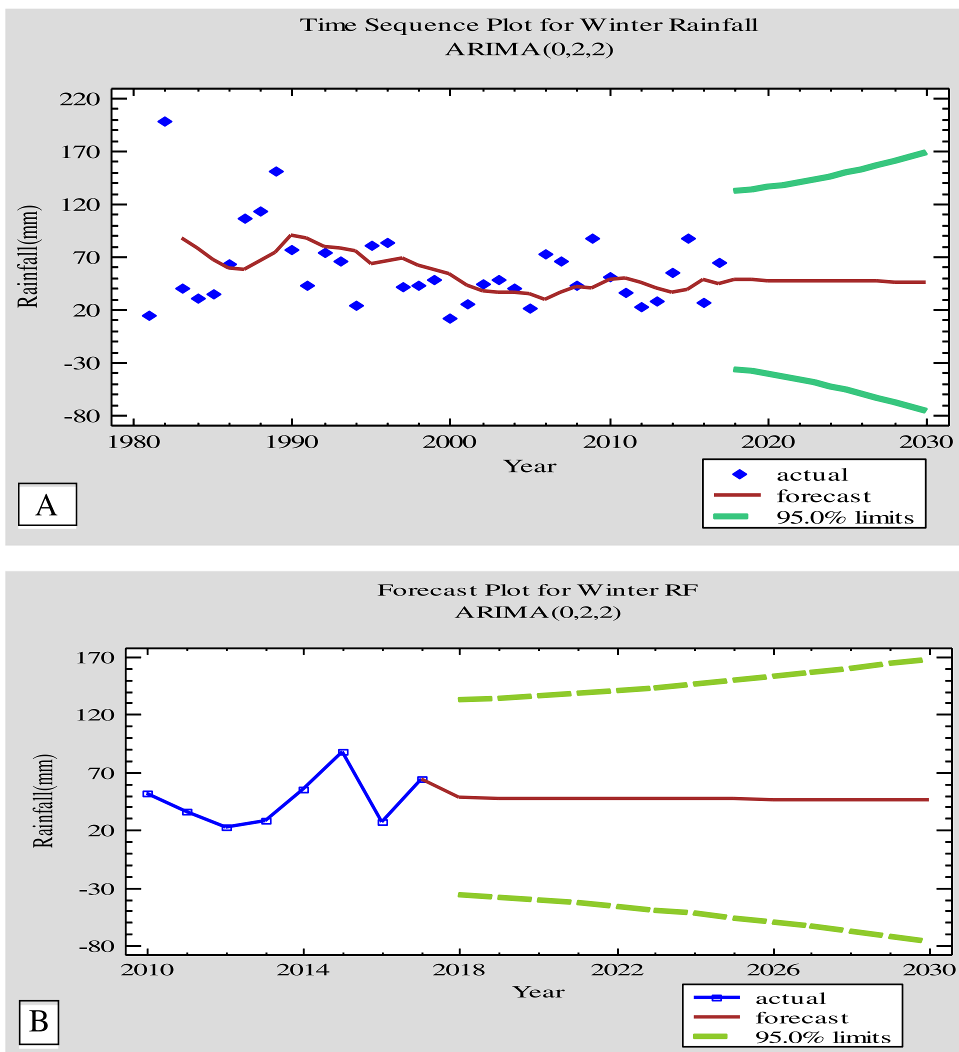

Fig. 3 Forecasted plots of winter rainfall

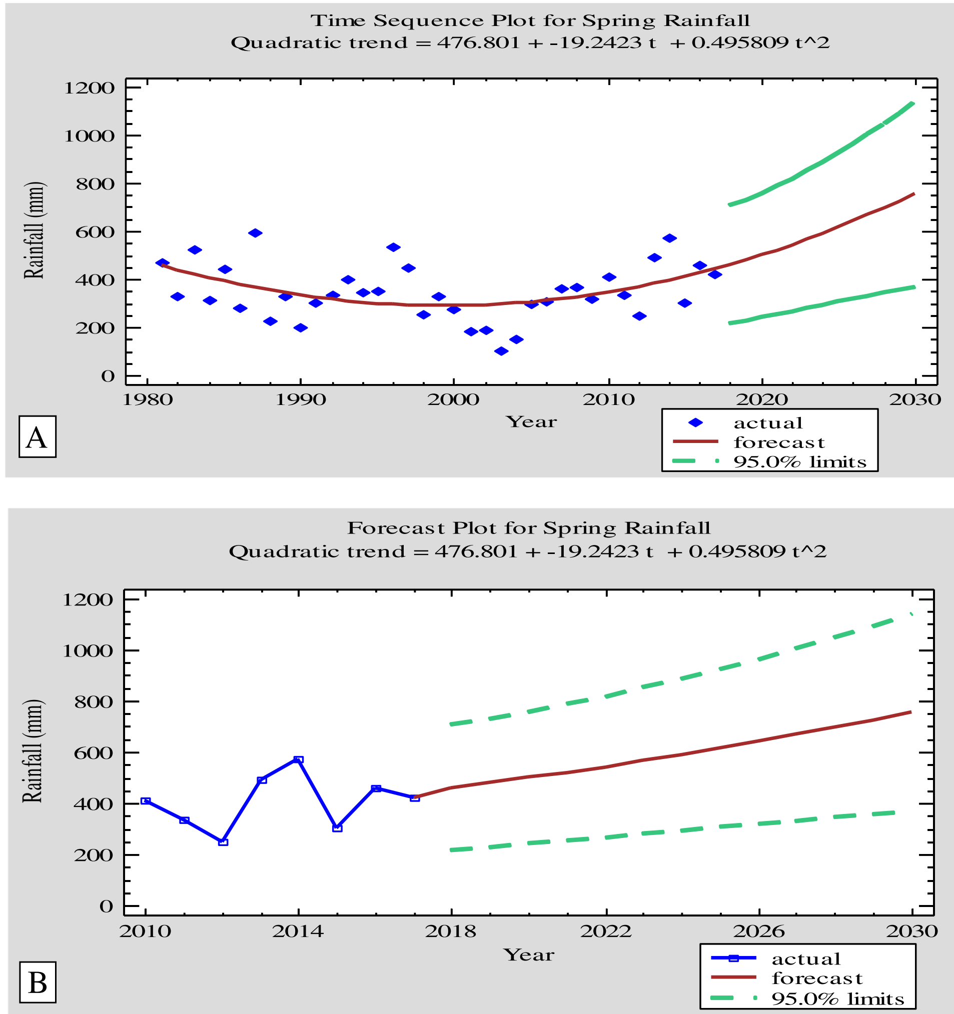

Fig. 4 Forecasted plots of spring rainfall

Table 3 ARIMA (2, 1, 2) model summary to forecast summer rainfall

Parameter	*Estimate*	*Stnd. error*	*t*	*P value*
AR(1)	−0.566914	0.0921083	−6.15486	0.000001
AR(2)	−0.919607	0.0904063	−10.1719	0.000000
MA(1)	−0.199438	0.0253705	−7.86099	0.000000
MA(2)	−0.973874	0.0386911	−25.1705	0.000000

fitted models. Figure 4B indicates forecasted plots of spring rainfall and for time periods beyond the end of the series shows 95% prediction limits for the forecasts. These limits show where the true data value at a selected future time is likely to be with 95% confidence level.

Summer rainfall time series forecasting

To forecast future values of summer rainfall, an autoregressive integrated moving average (ARIMA) model was selected. As indicated in Table 3, the output summarizes the statistical significance of the terms in the forecasting model. Terms with *P* values less than 0.05 are statistically significant at the 95% confidence level.

Forecast plot of summer rainfall

Figure 5 below indicates forecasted plots of summer rainfall. Figure 5A shows time sequence plot for summer rainfall with the predicted values when the actual data available from the fitted models. Figure 5B indicates forecasted plots of summer rainfall and for time periods beyond the end of the series shows 95% prediction limits for the forecasts. These limits show where the true data value at a selected future time is likely to be with 95% confidence level.

Autumn rainfall time series forecasting

To forecast future values of autumn rainfall, an autoregressive integrated moving average (ARIMA) model was selected. The output summarizes the statistical significance

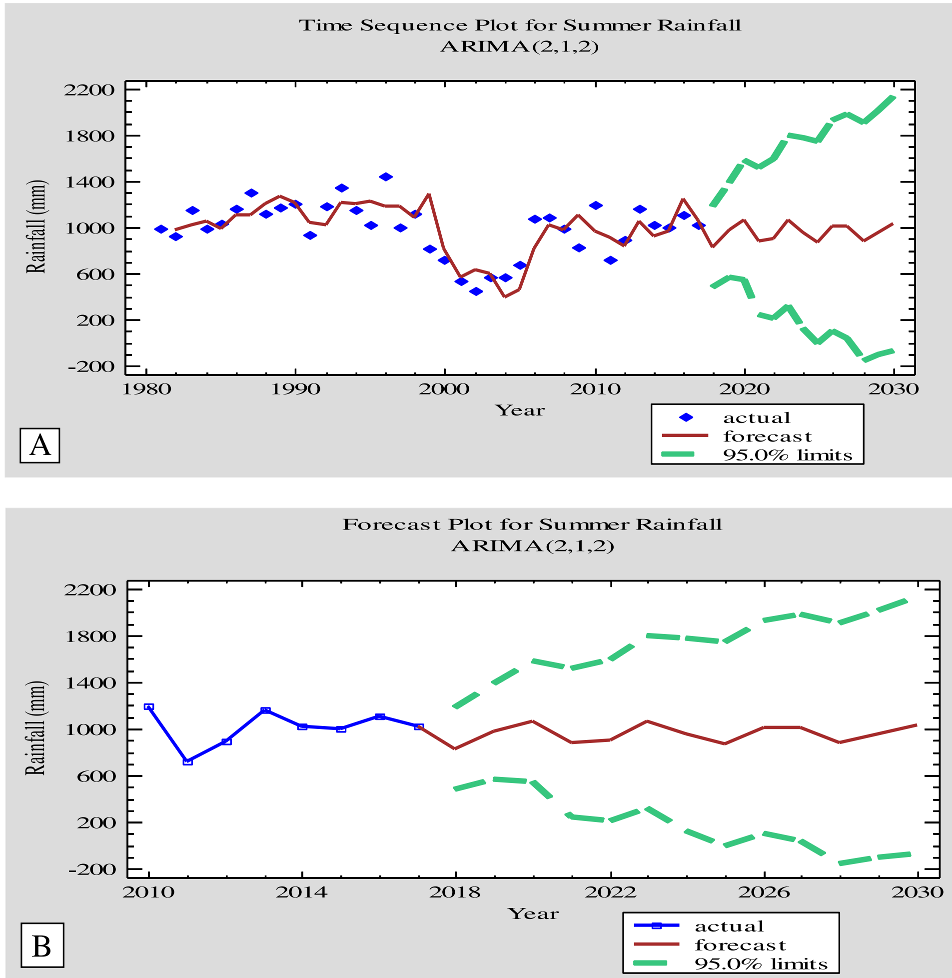

Fig. 5 Forecasted plots of summer rainfall

Table 4 ARIMA (2, 1, 2) model summary to forecast autumn rainfall

Parameter	*Estimate*	*Stnd. error*	*t*	*P value*
AR (1)	−0.527436	0.126142	−4.18129	0.000210
AR (2)	0.564844	0.149549	3.77699	0.000652
MA (1)	−0.00471918	0.108418	−0.0435277	0.965551
MA (2)	1.06644	0.124651	8.55537	0.000000

of the terms in the forecasting model. Terms with *P* values less than 0.05 are statistically significantly at the 95% confidence level. The *P* value for the AR (2) and MA (2) term is less than 0.05, so it is significantly significant. Table 4 below shows ARMA (2, 1, 2) model summary.

Forecast plot of autumn rainfall

Figure 6 below indicates forecasted plots of autumn rainfall. Figure 6A indicates time sequence plot for autumn rainfall with the predicted values when the actual data available from the fitted models. Figure 6B shows forecasted plots of autumn rainfall and for time periods beyond the end of the series shows 95% prediction limits for the forecasts. These limits show where the true data value at a selected future time is likely to be with 95% confidence level.

Trends of forecasted seasonal rainfall

The two-sided Mann–Kendall test was performed to examine whether there is a statistically significant monotonic increasing or decreasing trend in the forecasted seasonal rainfall as shown in Table 5. The result demonstrated a significant decreasing and increasing trend in the forecasted winter and spring rainfall respectively. An insignificant increasing and decreasing trend was detected in forecasted summer and autumn rainfall respectively. The Sen's slope of a trend line displays a declining magnitude in forecasted rainfall of winter and autumn while it shows an increased magnitude in the forecasted rainfall of spring and summer.

Winter minimum temperature time series forecasting

To forecast future values of winter minimum temperature, an autoregressive integrated moving average (ARIMA)

Fig. 6 Forecasted plots of autumn rainfall

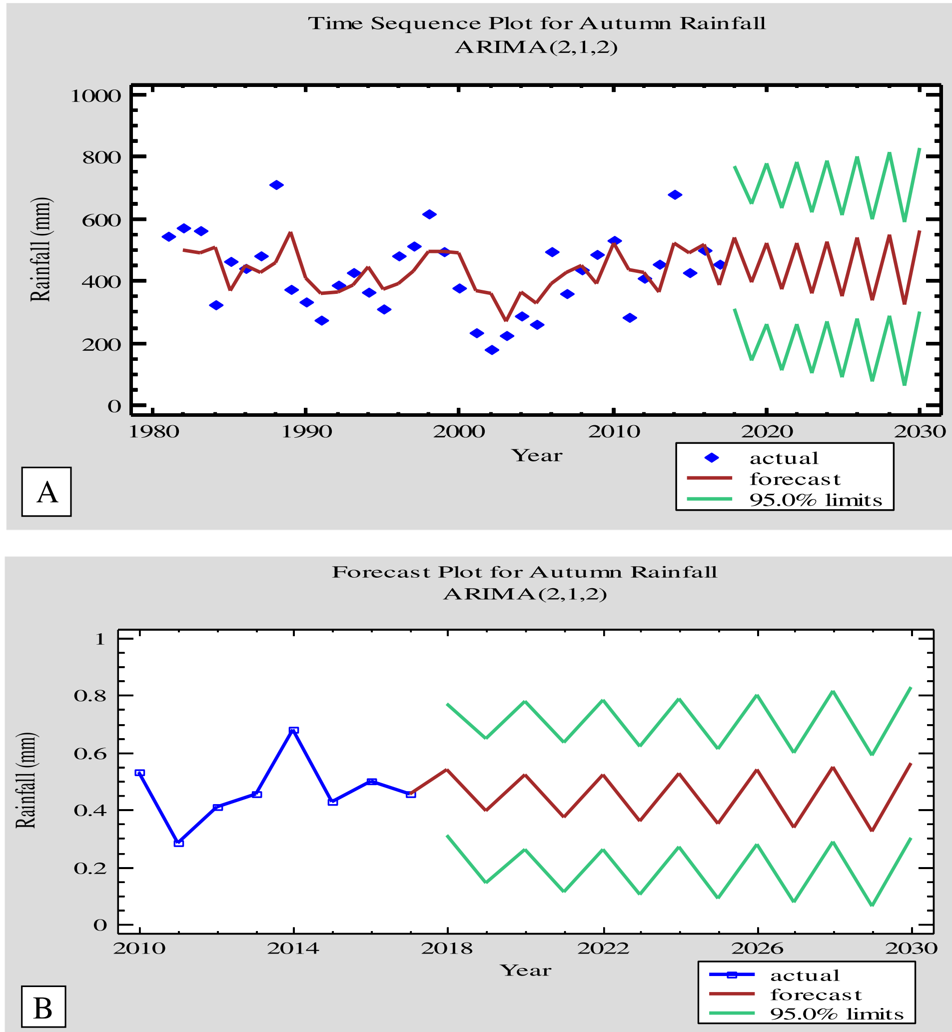

Table 5 Mann–Kendall trend test results for the forecasted seasonal rainfall

Season	MK stat (S)	Kendall's tau	*P* value (two-tailed)	Alpha (α)	Sen's slope	Trend (at 0.05 sig. level)
Winter	−78	−1	< 0.0001	0.05	−5.803	Significant
Spring	78	1	< 0.0001	0.05	0.041	Significant
Summer	10	0.128	0.590	0.05	0.011	Insignificant
Autumn	−2	−0.026	0.952	0.05	−0.005	Insignificant

P value of less than or equal to 0.05 is significant, while one more than 0.05 is not

model was employed. This model assumes that the best forecast for future data is given by a parametric model relating the most recent data value to previous data values and previous noise. The output summarizes the statistical significance of the terms in the forecasting model. Terms with *P* values less than 0.05 are statistically significantly at the 95% confidence level. Table 6 below indicates ARMA model summary for winter minimum temperature.

Table 6 ARIMA (0, 0, 1) model summary to forecast winter minimum temperature

Parameter	*Estimate*	*Stnd. error*	*t*	*P value*
MA (1)	−0.48679	0.160779	−3.02769	0.004604
Mean	13.1796	0.183799	71.7065	0.000000
Constant	13.1796			

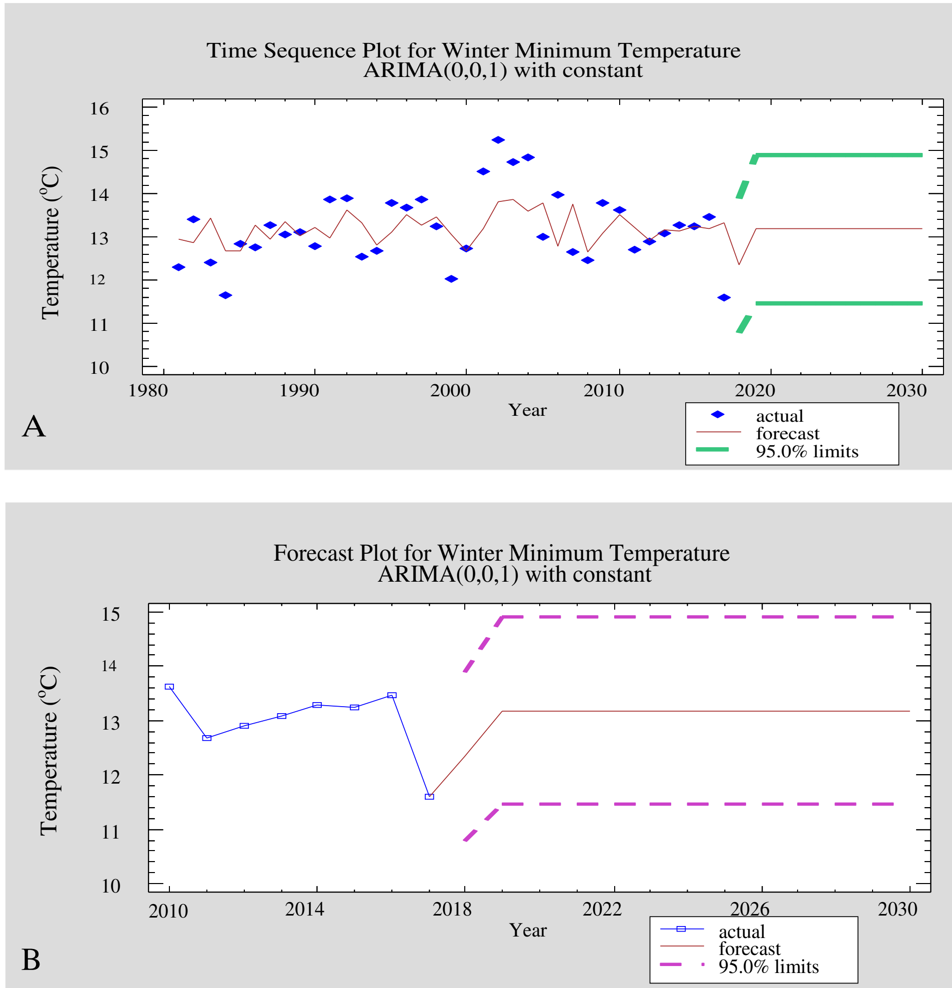

Fig. 7 Forecasted plots of winter minimum temperature

Forecast plot of winter minimum temperature

Figure 7 below indicates forecasted plots of winter minimum temperature. Figure 7A shows time sequence plot for winter minimum temperature with the predicted values when the actual data available from the fitted models. Figure 7B indicates forecasted plots of winter minimum temperature and for time periods beyond the end of the series shows 95% prediction limits for the forecasts. These limits show where the true data value at a selected future time is likely to be with 95% confidence level.

Spring minimum temperature time series forecasting

To forecast future values of spring minimum temperature, simple exponential smoothing model was selected. This model assumes that the best forecast for future data is given by an exponentially weighted average of all previous data values.

Forecast plot of spring minimum temperature

Figure 8 below indicates forecasted plots of spring minimum temperature. Figure 8A shows time sequence plot for spring minimum temperature with the predicted values when the actual data available from the fitted models. Figure 8B indicates forecasted plots of spring minimum temperature and for time periods beyond the end of the series shows 95% prediction limits for the forecasts. These limits show where the true data value at a selected future time is likely to be with 95% confidence level.

Summer minimum temperature time series forecasting

To forecast future values of summer minimum temperature, an autoregressive integrated moving average (ARIMA)

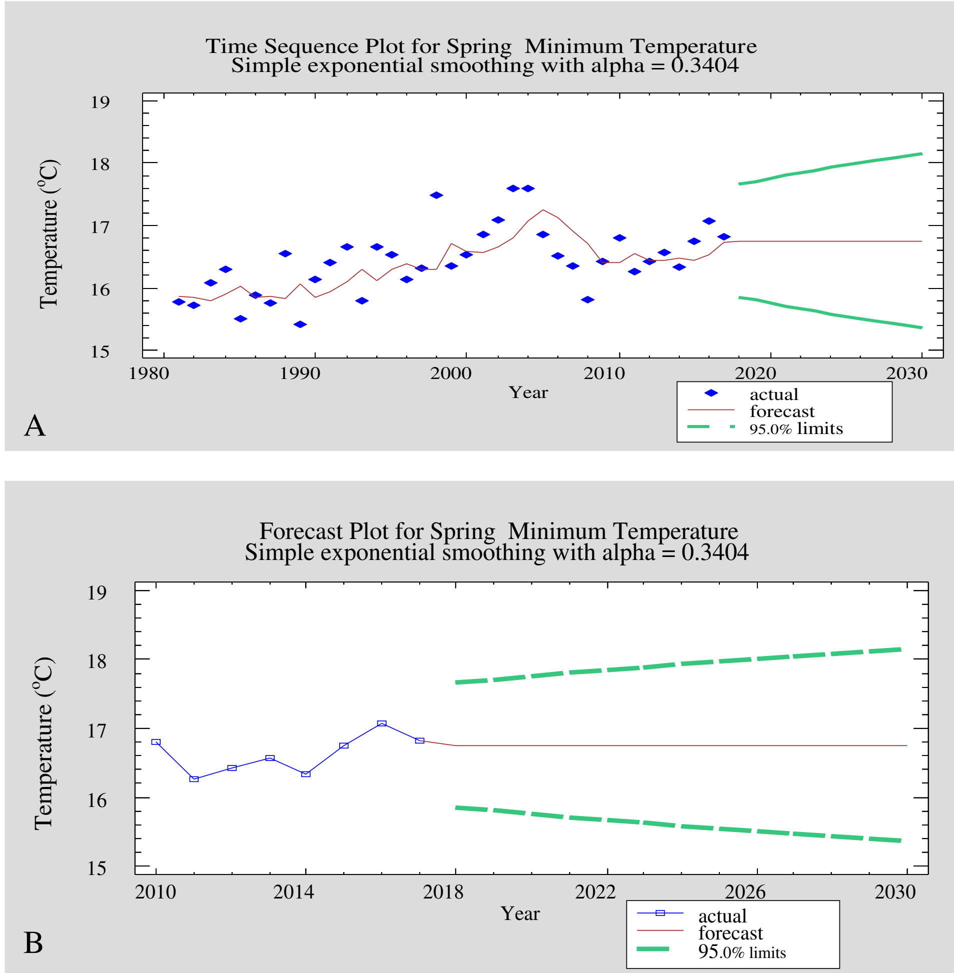

Fig. 8 Forecasted plots of spring minimum temperature

model was selected. This model assumes that the best forecast for future data is given by a parametric model relating the most recent data value to previous data values and previous noise. As indicated in Table 7, the output summarizes the statistical significance of the terms in the forecasting model. Terms with *P* values less than 0.05 are statistically significantly at the 95% confidence level. The *P* value for the AR (2) and MA (2) term is less than 0.05, so it is significantly significant.

Table 7 ARIMA (2, 1, 2) model summary to forecast summer minimum temperature

Parameter	*Estimate*	*Stnd. error*	*t*	*P value*
AR (1)	1.02999	0.167406	6.15262	0.000001
AR (2)	−0.530487	0.155283	−3.41626	0.001745
MA (1)	1.85233	0.0375653	49.3097	0.000000
MA (2)	−0.954703	0.0418472	−22.814	0.000000

Forecast plot of summer minimum temperature

Figure 9 below indicates forecasted plots of summer minimum temperature. Figure 9A shows time sequence plot for summer minimum temperature with the predicted values when the actual data available from the fitted models. Figure 9B indicates forecasted plots of summer minimum temperature and, for time periods beyond the end of the series, shows 95% prediction limits for the forecasts. These limits show where the true data value at a selected future time is likely to be with 95% confidence.

Autumn minimum temperature time series forecasting

To forecast future values of autumn minimum temperature, a linear trend model was selected. This model assumes that the best forecast for future data is given by a linear regression line fit to all previous data. The output summarizes the statistical significance of the terms in the forecasting

Fig. 9 Forecasted plots of summer minimum temperature

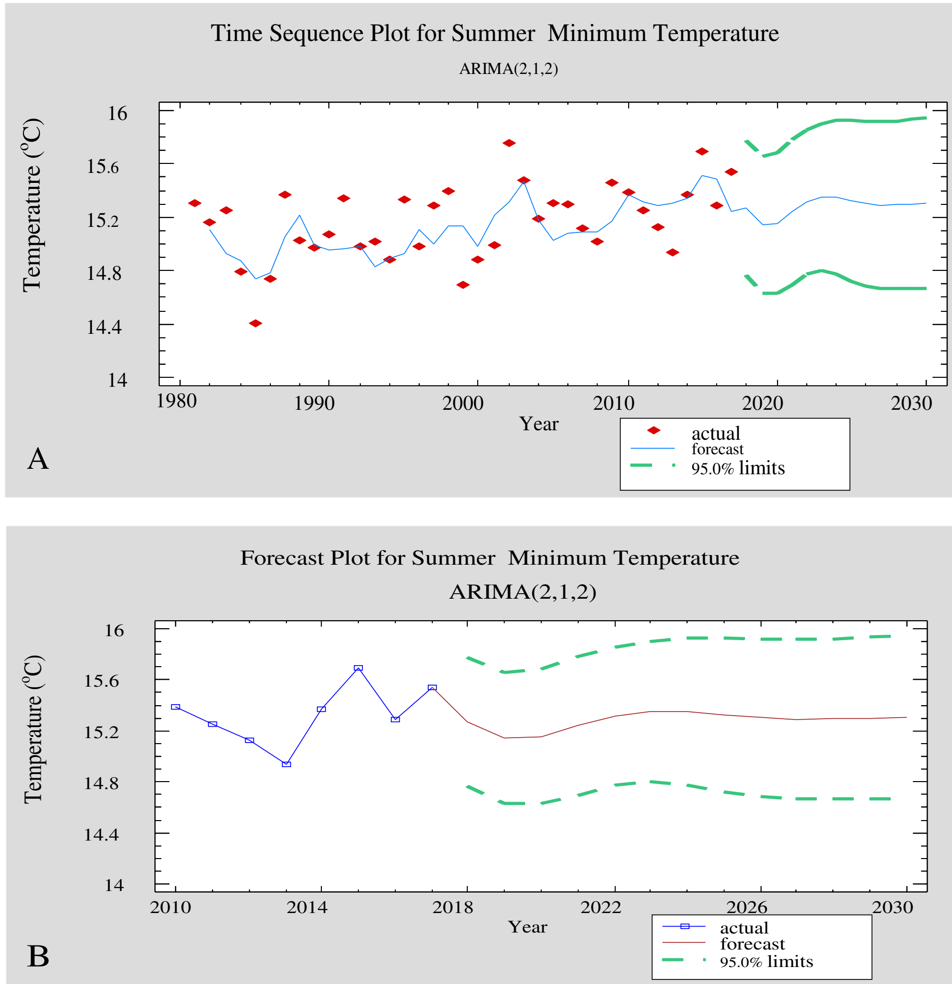

Table 8 Linear trend model summary to forecast autumn minimum temperature

Parameter	*Estimate*	*Stnd. error*	*t*	*P value*
Constant	13.0934	0.173939	75.2758	0.000000
Slope	0.0243717	0.00798089	3.05376	0.004300

model. Terms with *P* values less than 0.05 are statistically significantly at the 95% confidence level. In this case, the *P* value for the linear term is less than 0.05, so it is significantly significant. Table 8 below indicates linear trend model summary for autumn minimum temperature.

Forecast plot of autumn minimum temperature

Figure 10 below indicates forecasted plots of autumn minimum temperature. Figure 10A shows time sequence plot for autumn minimum temperature with the predicted values when the actual data available from the fitted models. Figure 10B indicates forecasted plots of autumn minimum temperature and for time periods beyond the end of the series shows 95% prediction limits for the forecasts. These limits show where the true data value at a selected future time is likely to be with 95% confidence.

Trends of forecasted seasonal minimum temperature

The two-sided Mann–Kendall test was performed to examine whether there is a statistically significant monotonic increasing or decreasing trend in the forecasted seasonal minimum temperature as shown in Table 9. The result revealed a significant increasing trend in the forecasted winter, spring, and autumn forecasted minimum temperature while it shows an insignificant upward trend for summer minimum temperature. The Sen's slope of a trend line exhibited an increased magnitude in the forecasted minimum temperature of winter, summer, and autumn while it shows a declining magnitude in the forecasted minimum temperature of spring.

Fig. 10 Forecasted plots of autumn minimum temperature

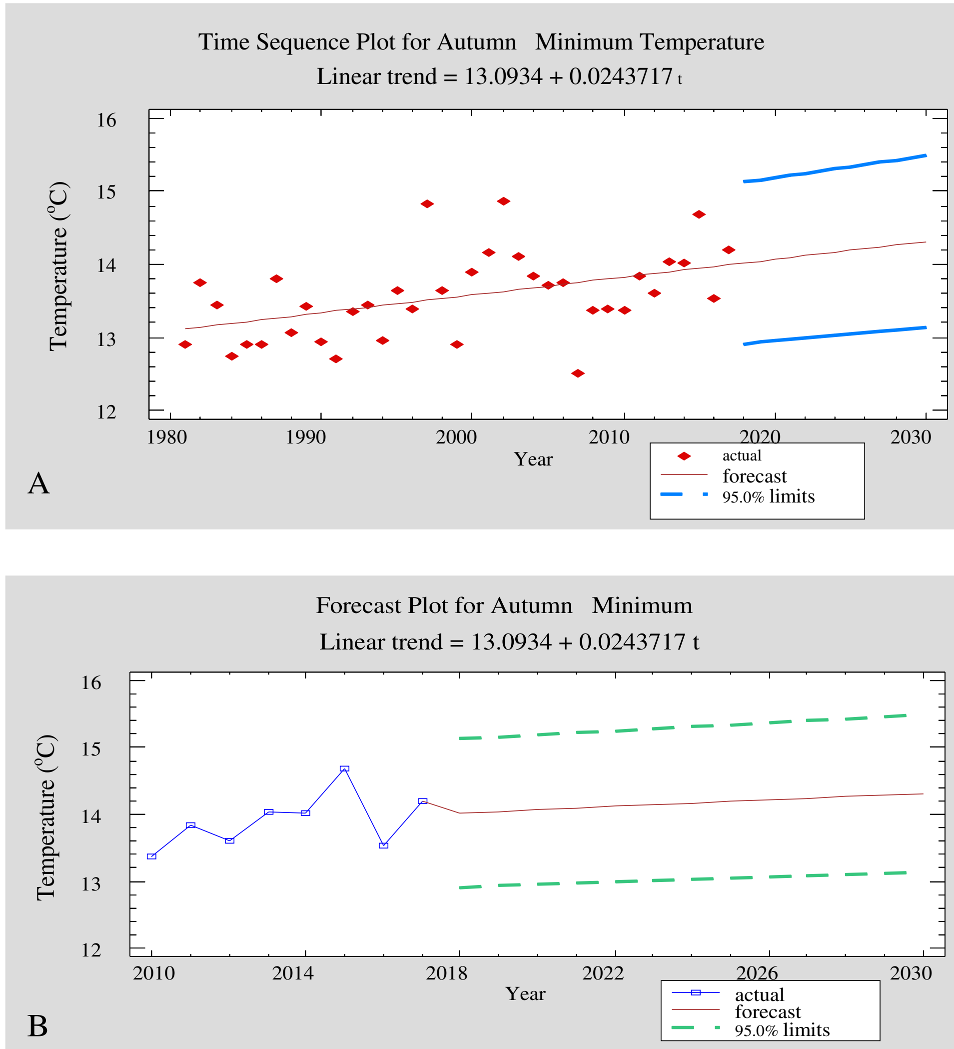

Table 9 Mann–Kendall trend test results for the forecasted seasonal minimum temperature

Season	MK Stat (S)	Kendall's tau	*P* value (two-tailed)	Alpha (α)	Sen's slope	Trend (at 0.05 sig. level)
Winter	78	1	< 0.0001	0.05	7.738	Significant
Spring	78	1	< 0.0001	0.05	− 0.500	Significant
Summer	20	0.256	0.252	0.05	26.110	Insignificant
Autumn	78	1	< 0.0001	0.05	41.026	Significant

Table 10 ARIMA (0, 2, 1) model summary to forecast winter maximum temperature

Parameter	*Estimate*	*Stnd. Error*	*t*	*P value*
MA(1)	1.02366	0.0169411	60.4247	0.000000

Winter maximum temperature time series forecasting

To forecast future values of winter maximum temperature, an autoregressive integrated moving average (ARIMA) model was selected. This model assumes that the best forecast for future data is given by a parametric model relating the most recent data value to previous data values and previous noise. As indicated in Table 10 below the output summarizes the statistical significance of the terms in the forecasting model. Terms with *P* values less than 0.05 are statistically significantly at the 95% confidence level.

Forecast plot of winter maximum temperature

Figure 11 below indicates forecasted plots of winter maximum temperature. Figure 11A shows time sequence plot

Fig. 11 Forecasted plots of winter maximum temperature

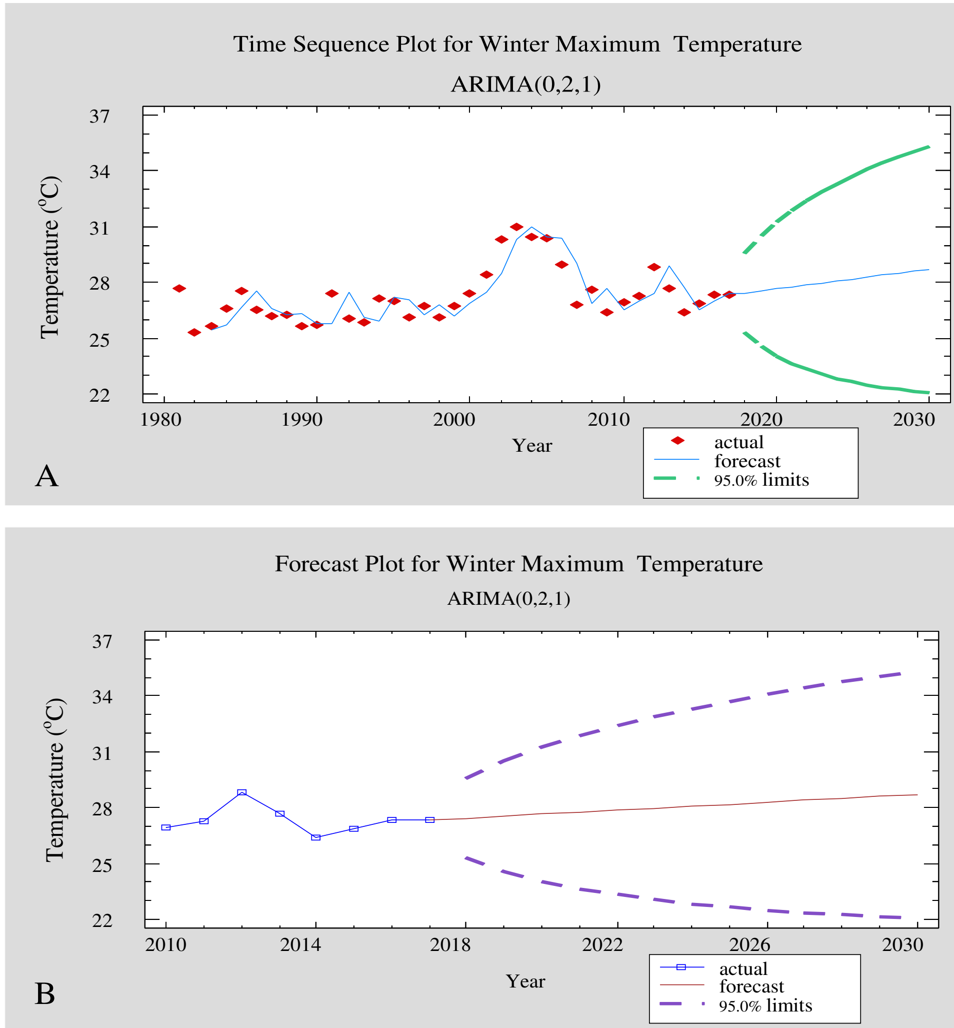

for winter maximum temperature with the predicted values when the actual data available from the fitted models. Figure 11B indicates forecasted plots of winter maximum temperature and for time periods beyond the end of the series shows 95% prediction limits for the forecasts. These limits show where the true data value at a selected future time is likely to be with 95% confidence.

Spring maximum temperature time series forecasting

To forecast future values of spring maximum temperature, simple exponential smoothing model was selected. This model assumes that the best forecast for future data is given by an exponentially weighted average of all previous data values.

Forecast plot of spring maximum temperature

Figure 12 below indicates forecasted plots of spring maximum temperature. Figure 12A shows time sequence plot for spring maximum temperature with the predicted values when the actual data available from the fitted models. Figure 12B indicates forecasted plots of spring maximum temperature, and for time periods beyond the end of the series, it shows 95% prediction limits for the forecasts. These limits show where the true data value at a selected future time is likely to be with 95% confidence.

Summer maximum temperature time series forecasting

To forecast future values of summer maximum temperature, an autoregressive integrated moving average (ARIMA) model was employed. This model assumes that the best forecast for future data is given by a parametric model relating the most recent data value to previous data values and previous noise. As indicated in Table 11, the output summarizes the statistical significance of the terms in the forecasting

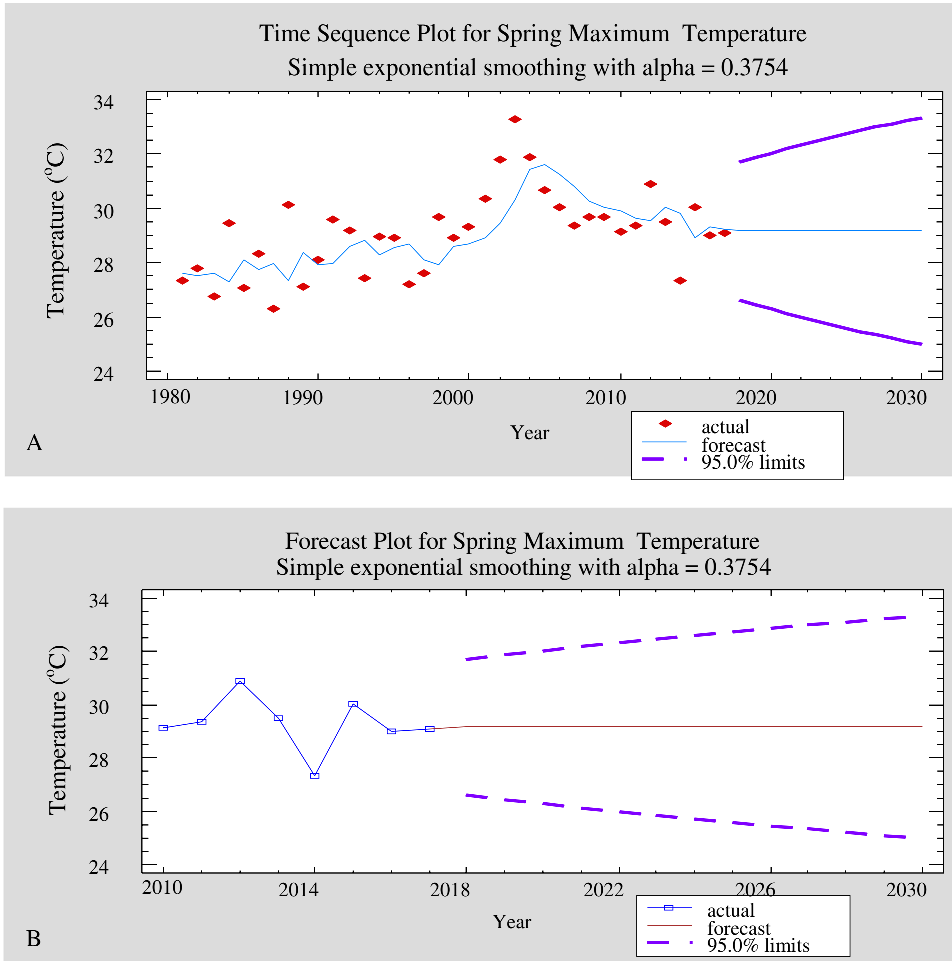

Fig. 12 Forecasted plots of spring maximum temperature

Table 11 ARIMA (1, 0, 0) model summary to forecast summer maximum temperature

Parameter	*Estimate*	*Stnd. Error*	*t*	*P value*
AR (1)	0.443807	0.154235	2.87746	0.006788
Mean	22.6683	0.148988	152.149	0.000000
Constant	12.608			

model. Terms with P-values less than 0.05 are statistically significantly at the 95% confidence level.

Forecast plot of summer maximum temperature

Figure 13 below indicates forecasted plots of summer maximum temperature. Figure 13A shows time sequence plot for summer maximum temperature with the predicted values when the actual data available from the fitted models. Figure 13B indicates forecasted plots of summer maximum temperature and, for time periods beyond the end of the series, shows 95% prediction limits for the forecasts. These limits show where the true data value at a selected future time is likely to be with 95% confidence.

Autumn maximum temperature time series forecasting

To forecast future values of autumn maximum temperature, an autoregressive integrated moving average (ARIMA) model was employed. This model assumes that the best forecast for future data is given by a parametric model relating the most recent data value to previous data values and previous noise. The output summarizes the statistical significance of the terms in the forecasting model. Terms with *P* values less than 0.05 are statistically significantly at the 95% confidence level. The *P* value for the AR (1) term is less than 0.05. Table 12 below shows ARIMA model summary for autumn maximum temperature.

Forecast plot of autumn maximum temperature

Figure 14 below indicates forecasted plots of autumn maximum temperature. Figure 14A shows time sequence plot for autumn maximum temperature with the predicted values when the actual data available from the fitted models. Figure 14B indicates forecasted plots of autumn maximum

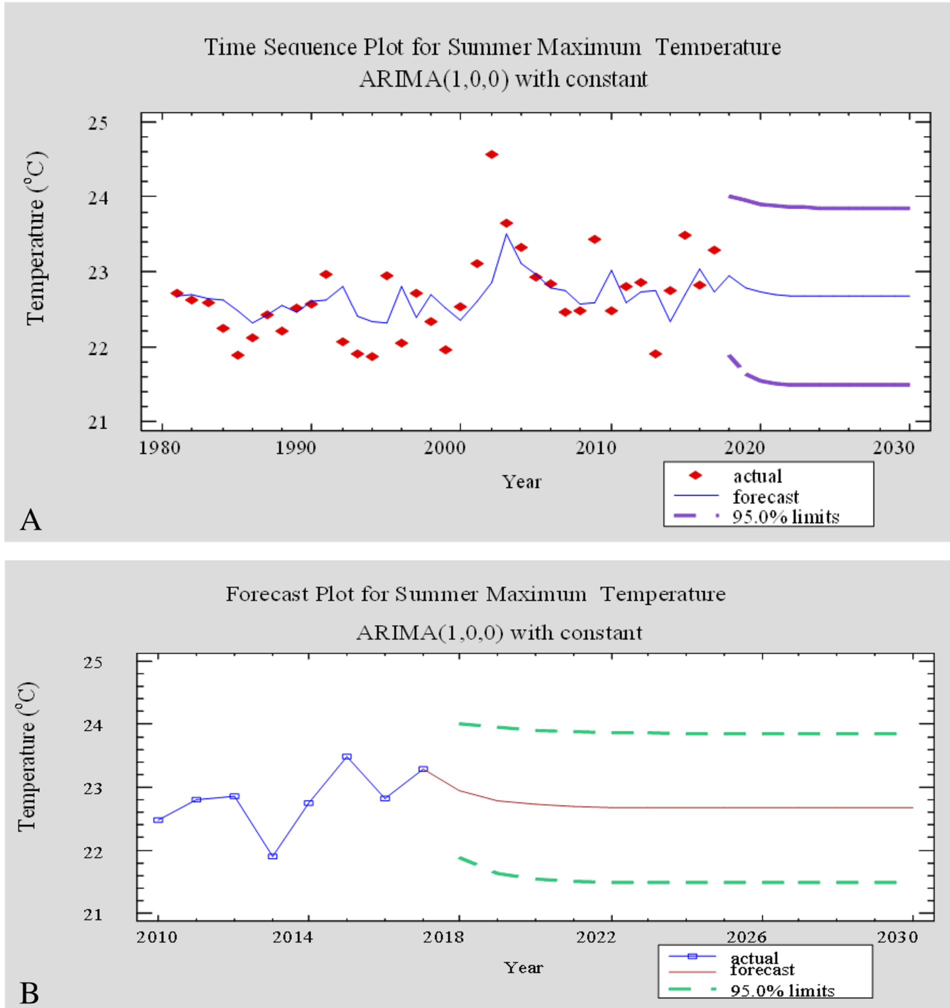

Fig. 13 Forecasted plots of summer maximum temperature

Table 12 ARIMA (1, 0, 0) model summary to forecast autumn maximum temperature

Parameter	*Estimate*	*Stnd. error*	*t*	*P value*
AR (1)	0.651373	0.127846	5.09496	0.000012
Mean	24.064	0.292108	82.3806	0.000000
Constant	8.38938			

temperature and, for time periods beyond the end of the series, shows 95% prediction limits for the forecasts. These limits show where the true data value at a selected future time is likely to be with 95% confidence.

Trends of forecasted seasonal maximum temperature

The two-sided Mann–Kendall test was performed to examine whether there is a statistically significant monotonic increasing or decreasing trend in the forecasted seasonal maximum temperature as shown in Table 13. The result revealed a significant increasing trend in the forecasted winter and spring forecasted maximum temperature while it shows a significant declining trend for the forecasted summer and autumn maximum temperature. The Sen's slope of a trend line exhibited an increased magnitude in the forecasted maximum temperature of winter, while it shows a declining magnitude in the forecasted maximum temperature of spring, summer and autumn.

Annual rainfall time series forecasting

To forecast future values of annual rainfall, an autoregressive integrated moving average (ARIMA) model has been selected based on its performance. This model assumes that the best forecast for future data is given by a parametric model relating the most recent data value to previous data values and previous noise. As indicated in Table 14 below, the output of the model was found to be statistically significant with *P* values less than 0.05 at the 95% confidence level. The *P* value for the

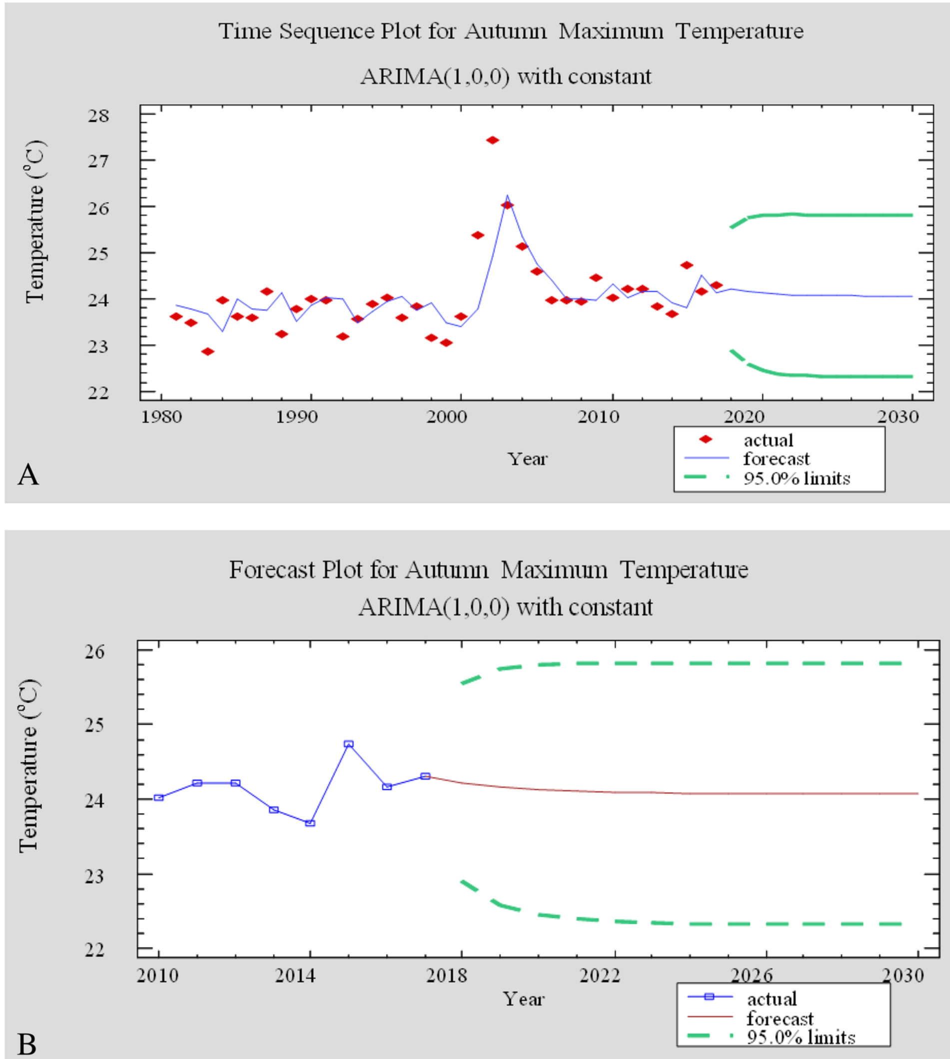

Fig. 14 Forecasted plots of autumn maximum temperature

Table 13 Mann–Kendall trend test results for the forecasted seasonal maximum temperature

Season	MK Stat (S)	Kendall's tau	*P* value (two-tailed)	Alpha (α)	Sen's slope	Trend (at 0.05 sig. level)
Winter	78	1	< 0.0001	0.05	9.444	Significant
Spring	78	1	< 0.0001	0.05	− 0.500	Significant
Summer	− 76	− 0.974	< 0.0001	0.05	− 213.675	Significant
Autumn	− 78	− 1	< 0.0001	0.05	− 145.423	Significant

Table 14 ARIMA (1, 0, 0) model summary to forecast annual rainfall

Parameter	Estimate	Stnd. error	*t*	*P* value
AR(1)	0.603771	0.134483	4.48955	0.000074
Mean	1831.06	133.89	13.6758	0.000000
Constant	725.521			

AR (1) and the *P* value for the constant term is less than 0.05, so it is significant at the 95% confidence level.

Forecast plot of annual rainfall

Figure 15 below indicates forecasted plots of annual rainfall. Figure 15A indicates time sequence plot for annual rainfall with the predicted values when the actual data available from the fitted models. Figure 15B shows forecasted plots of annual rainfall, and

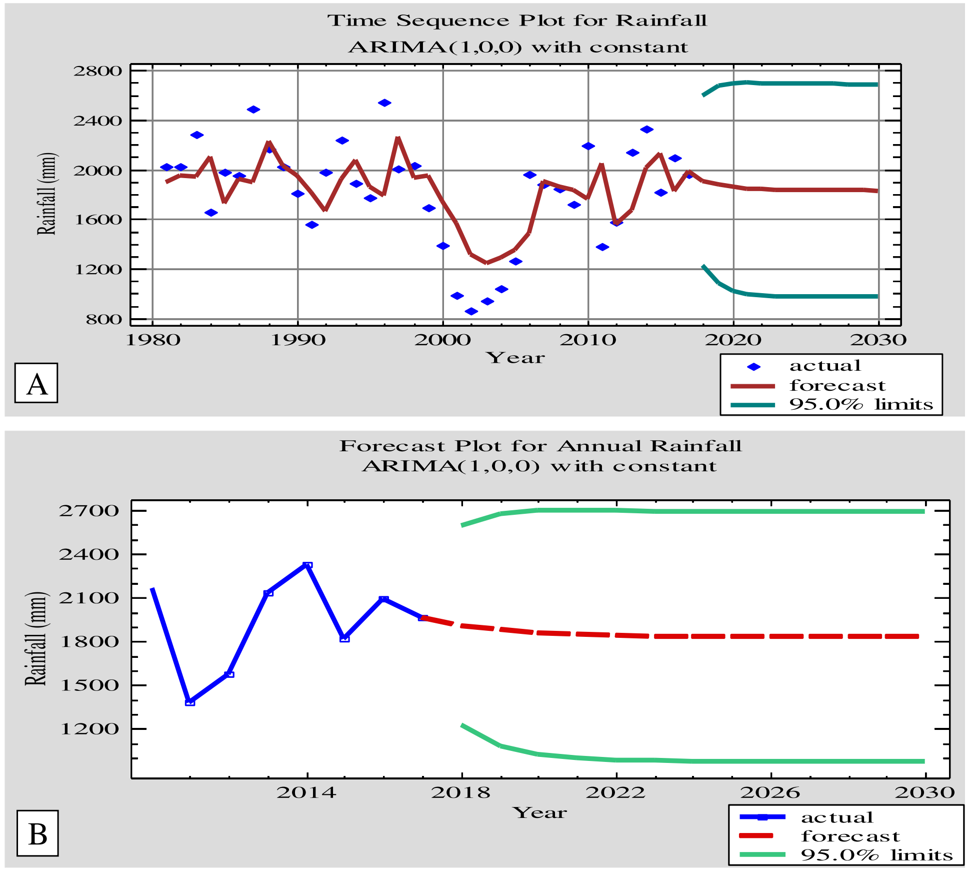

Fig. 15 Forecasted plots of annual rainfall

for time periods beyond the end of the series, it shows 95% prediction limits for the forecasts. These limits show where the true data value at a selected future time is likely to be with 95% confidence, assuming the fitted model was appropriate for the data.

Annual maximum temperature time series forecasting

To forecast annual maximum temperature to the future based on the actual historical value, an autoregressive integrated moving average (ARIMA) model has been selected. This model assumes that the best forecast for future data is given by a parametric model relating the most recent data value to previous data values and previous noise. The output summarizes the statistical significance of the terms in the forecasting model. Values with *P* values less than 0.05 are statistically significant at the 95% confidence level. The *P* value for the AR (1) and MA (1) was statistically significant to use the model. Table 15 below also summarizes the performance of the currently selected model in fitting the historical data.

Forecast plot for annual maximum temperature

Figure 16 below indicates forecasted plots of annual maximum temperature. Figure 16A shows time sequence plots of annual maximum temperature with the predicted values when the actual data available from the fitted models. Figure 16B indicates forecasted annual maximum temperature, and the time periods beyond the end of the series show 95% prediction limits for the forecasts. These limits show where the true data value at a selected future time is likely to be with 95% confidence, assuming the fitted model is appropriate for the data.

Table 15 ARIMA (1, 1, 1) model summaries for annual maximum temperature

Parameter	Estimate	Stnd. error	*t*	*P* value
AR (1)	0.692153	0.123729	5.59412	0.000003
MA (1)	1.09559	0.00068835	1591.61	0.000000

Trends of forecasted annual rainfall and temperature

The two-sided Mann–Kendall test was performed to examine whether there is a statistically significant monotonic increasing or decreasing trend in the forecasted annual rainfall and temperature as shown in Table 16. The result revealed a significant increasing trend in the forecasted annual minimum

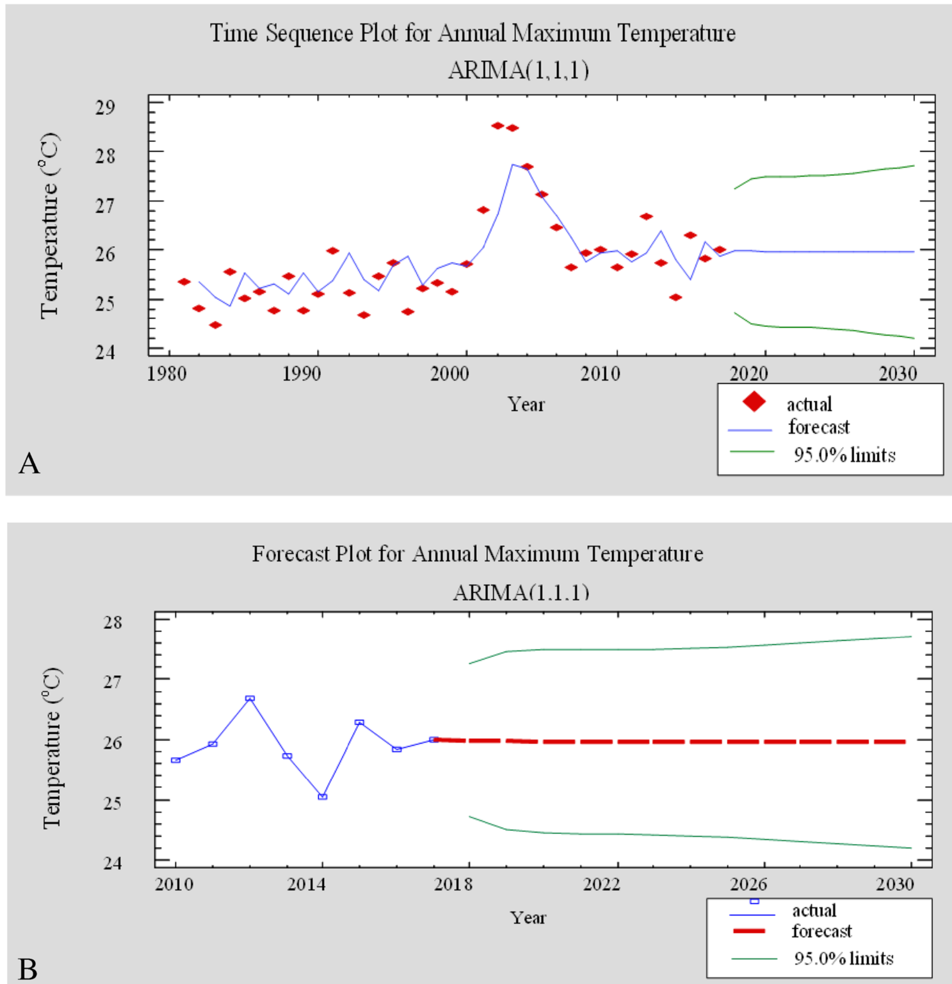

Fig. 16 Forecasted plots of annual maximum temperature

Table 16 Mann–Kendall trend test results for the forecasted annual rainfall and temperature

Annual	MK Stat (S)	Kendall's tau	*P* value (two-tailed)	Alpha (α)	Sen's slope	Trend (at 0.05 sig. level)
Rainfall	−78	−1	< 0.0001	0.05	−0.329	Significant
Tmin	78	1	< 0.0001	0.05	980.392	Significant
Tmax	−78	−1	< 0.0001	0.05	−523.274	Significant

temperature while it shows a significant declining trend for annual rainfall and maximum temperature. The Sen's slope of a trend line exhibited an increased magnitude in the forecasted annual minimum temperature, while it shows a declining magnitude in the forecasted annual rainfall and maximum temperature. A study conducted in north central Ethiopia also revealed an increasing trend for minimum average temperatures (Asfaw et al. 2018). Another study also found a similar result of a declining trend in annual rainfall (Gemeda et al. 2021).

Conclusion

Ethiopia is one of the most vulnerable countries experiencing food insecurity as a result of crop damage by climate variability and change. Climate variability is already posing a serious obstacle to efforts of ensuring food security in the face of climate change. Farmers use their indigenous knowledge for weather and climate prediction to make farming decisions. Because of the complexities of climate change, relying on such unreliable information to sustainably enhance agricultural productivity and provide food security in a changing climate is difficult. Scientific based reliable climate information helps the farmers for building resilience to climate shocks by formulating appropriate adaptation strategies and crop management decisions. Knowledge about past and upcoming of weather and climate is very crucial for successful farm management. As a result, the study aimed to forecast rainfall and temperature so that farmers and agricultural planners could make informed adaptation decisions in advance. The predicted results for winter and spring rainfall indicated a significant decreasing and increasing tendency respectively. Summer and autumn rainfall exhibited an insignificant upward and downward trend respectively, but yearly rainfall showed a substantial declining trend. The projected winter, spring, autumn, and yearly minimum temperatures all indicate a considerable upward tendency, whereas the summer minimum temperature shows a negligible upward trend. The forecasted maximum temperature in the winter and spring shows a significant rising tendency, while in the summer, autumn, and annual shows a substantial dropping trend. As the livelihoods of the farmers mainly depend on seasonal rain fed agriculture, adapting to the adverse impact of rainfall and temperature variability is undisputable. Decisions regarding the agricultural system and formulation of adaptation strategies in the area are better to consider increasing in minimum temperature and declining in annual rainfall.

Declarations

Ethics approval This material is the authors' own original work, which has not been previously published elsewhere and not currently being considered for publication elsewhere.

Consent for publication We give our consent for this manuscript to be published in the Arabian Journal of Geosciences.

Conflict of interest The authors declare that they have no competing interests.

References

Achalu C (2014) Assessment of the severity of acid saturations on soils collected from cultivated lands of East Wollega Zone, Ethiopia. Star J 3(4):42–48

Akaike H (1973) Maximum likelihood identification of Gaussian autoregressive moving average models. Biometrika 60(2):255–265

Acquah HD-G (2018) Weighted average information criterion for selection of an asymmetric price relationship. Alanya Akademik Bakış 2(2):147–155. https://doi.org/10.29023/alanyaakademik.343737

Asamenew T, Mezene W (2015) Study on prevalence of poultry coccidiosis in Nekemte, town, East Wollega, Ethiopia. Afr J Agric Res 10(5):328–333. https://doi.org/10.5897/AJAR2013.6946

Asfaw A, Simane B, Hassen A, Bantider A (2018) Variability and time series trend analysis of rainfall and temperature in northcentral Ethiopia: a case study in Woleka sub-basin. Weather Clim Extremes 19(1):29–41. https://doi.org/10.1016/j.wace.2017.12.002

Cheung WH, Senay GB, Ashbindu S (2008) Trends and spatial distribution of annual and seasonal rainfall in Ethiopia. Int J Climatol 28:1723–1734. https://doi.org/10.1002/joc

Conway D, Schipper ELF (2011) Adaptation to climate change in Africa: challenges and opportunities identified from Ethiopia. Glob Environ Chang 21(1):227–237. https://doi.org/10.1016/j.gloenvcha.2010.07.013

Degefa K, Biru G, Abebe G (2020) Farming system characterization and analysis of East Wollega Zone, Oromia, Ethiopia. Int J Manag Fuzzy Syst 6(2):14–28. https://doi.org/10.11648/j.ijmfs.20200602.11

Dereje A, Tadesse B, Dejene N (2014) Prevalence of bovinetrypanosomiasis and associated risk factors in East Wollega Zone, Western Ethiopia. Eur J Biol Sci 6(2):1–8. https://doi.org/10.5829/idosi.ejbs.2014.6.02.85108

Diro GT, Black E, Grimes DIF (2008) Seasonal forecasting of Ethiopian spring rains. Meteorol Appl: a Journal of Forecasting, Practical Applications, Training Techniques and Modelling 15(1):73–83

EWZPEDO (2017) East Wollega Zone planning and economic development office: physical and socioeconomic profile of East Wollega Zone

Fita T (2014) White Mango Scale, Aulacaspis tubercularis, distribution and severity status in East and West Wollega Zones Western Ethiopia. Star J 3(3):1–10

Gbangou T, Sarku R, Van Slobbe E, Ludwig F, Kranjac-Berisavljevic G, Paparrizos S (2020) Coproducing weather forecast information with and for smallholder farmers in Ghana: evaluation and design principles. Atmosphere, 11(9). https://doi.org/10.3390/atmos11090902

Gebissa Y (2021) The challenges and prospects of Ethiopian agriculture. Cogent Food Agri 7(1). https://doi.org/10.1080/23311932.2021.1923619

Gemeda DO, Korecha D, Garedew W (2021) Evidences of climate change presences in the wettest parts of southwest Ethiopia. Heliyon 7(9):e08009. https://doi.org/10.1016/j.heliyon.2021.e08009

Kotir JH (2011) Climate change and variability in Sub-Saharan Africa: a review of current and future trends and impacts on agriculture and food security. Environ Dev Sustain 13(3):587–605

Mekasha A, Tesfaye K, Duncan AJ (2014) Trends in daily observed temperature and precipitation extremes over three Ethiopian ecoenvironments. Int J Climatol 34(6):1990–1999. https://doi.org/10.1002/joc.3816

Melese G (2019) Farmer's response to climate change and variability in Ethiopia: a review. Cogent Food Agric 5(1):1613770

Muhammad A, Michael K, Andrew W, Mansour A, Muhammad I, Tufa D, Nachiketa A, Asher S, Jemal S, Asaminew T (2021) Seasonal predictability of Ethiopian Kiremt rainfall and forecast skill of ECMWF's SEAS5 model. Clim Dyn 57(11–12):3075–3091. https://doi.org/10.1007/s00382-021-05855-0

Musayev S, Mellor J, Walsh T, Anagnostou E (2021) Development of an agent-based model for weather forecast information exchange in rural area of Bahir Dar, Ethiopia. Sustainability 13(9):4936

Omondi PAO, Awange JL, Forootan E, Ogallo LA, Barakiza R, Girmaw GB, Fesseha I, Kululetera V, Kilembe C, Mbati MM, Kilavi M, King'uyu SM, Omeny PA, Njogu A, Badr EM, Musa TA, Muchiri P, Bamanya D, Komutunga E (2014) Changes in temperature and precipitation extremes over the Greater Horn of Africa region from 1961 to 2010. Int J Climatol 34(4):1262–1277. https://doi.org/10.1002/joc.3763

Radeny M, Desalegn A, Mubiru D, Kyazze F, Mahoo H, Recha J, ... Solomon D (2019) Indigenous knowledge for seasonal weather and climate forecasting across East Africa. Clim Change 156(4) 509-526

Rosell S (2011) Regional perspective on rainfall change and variability in the central highlands of Ethiopia, 1978–2007. Appl Geogr 31(1):329–338

Singh SN (2019) Climate change and agriculture in Ethiopia: a case study of Mettu Woreda. SocioEconomic Challenges 3(3):61–79. https://doi.org/10.21272/sec.3(3).61-79.2019

Sintayehu A (2018) Application of time series analysis to annual rainfall values in Debre Markos Town, Ethiopia. Comput Water, Energy, Environ Eng 7(03):81

Tesfahun B, Nurilign S, Gurju A, Tesfaye K (2018) Modeling and forecasting rainfall in Ethiopia. Int J Comput Sci Appl Math 4(2):42. https://doi.org/10.12962/j24775401.v4i2.3824

Teshome H (2020) Time series analysis of monthly average temperature and rainfall using seasonal ARIMA model (in case of Ambo Area, Ethiopia). Int J Theor Appl Math 6(5):76–87. https://doi.org/10.11648/j.ijtam.20200605.13

Wagaye B, Endalamaw W, Lubaba M, Yimer M, Hassen A, Yilma D (2020) Assessing the impact of rainfall variability on teff production and farmers perception at Gubalafto District, North Eastern, Ethiopia. Int J Earth Sci Geophys 6(2). https://doi.org/10.35840/2631-5033/1842

Wagesho N, Goel NK, Jain MK (2013) Temporal and spatial variability of annual and seasonal rainfall over Ethiopia. Hydrol Sci J 58(2):354–373. https://doi.org/10.1080/02626667.2012.754543

Wasihun G, Desu A (2021) Trend of cereal crops production area and productivity Ethiopia. J Cereals Oilseeds 12(1):9–17. https://doi.org/10.5897/jco2020.0206

Workalemahu S, Dawid I (2021) Smallholder farmers ' adaptation strategies, opportunities and challenges to climate change : a review. Int J Food Sci Agric 5(4):592–600. https://doi.org/10.26855/ijfsa.2021.12.005

Yate T, Hutjes R (2021) Assessing the potential of using ECMWF system-4 seasonal rainfall forecasts over Central-West Ethiopia. Climatol Weather Forecast OPEN 9(3):1–9